

# Detectors for next-generation quasi-free scattering experiments

Junki Tanaka<sup>1,2</sup>, Martha Liliana Cortés<sup>2</sup>, Hongna Liu<sup>3</sup>, and Ryo Taniuchi<sup>4</sup>

<sup>1</sup>*RCNP, Osaka University, 10-1 Mihogaoka, Ibaraki, Osaka, Japan*

<sup>2</sup>*RIKEN Nishina Center, 2-1 Hirosawa, Wako, Saitama 351-0198, Japan*

<sup>3</sup>*Key Laboratory of Beam Technology of Ministry of Education, College of Nuclear Science and Technology, Beijing Normal University, Beijing 100875, China*

<sup>4</sup>*School of Physics, Engineering and Technology, University of York, York, YO10 5DD, United Kingdom*

.....  
 Quasi-free scattering of atomic nuclei away from the stability line has reached several milestones over the past decade. The advent of gamma, charged particles, and neutron detection devices for inverse kinematics, especially in combination with RI beams, has opened new horizons in nuclear physics. Research is progressing with detection devices optimized to explore these new and challenging area of physics. While some of the new detection developments aim for high energy and angular resolution, others focus on the increasing detection efficiency or enhancing large angular acceptance. As high-intensity RI beams become available worldwide, we reflect on past detectors and provide a review of the future development of the detection devices.

.....  
 Subject Index      xxx, xxx

# 1 Introduction

The Radioactive Isotope Beam Factory (RIBF) at the RIKEN Nishina Center utilizes a variety of advanced detection systems, including DALI2 [1] and NEBULA [2], which play a crucial role in exploring the structure and behavior of atomic nuclei. Additionally, external devices such as MINOS [3] are often employed in collaborative experiments to enhance the facility's experimental capabilities.

MINOS utilizes a cylindrical liquid hydrogen ( $\text{LH}_2$ ) target, with a maximum length of 150 mm along the beam axis, designed to enhance luminosity. This setup is particularly useful for studying exotic species produced at low count rates. Surrounding the target is a time projection chamber (TPC), which plays a key role in reconstructing the reaction vertex and identifying the reaction process. DALI2, an array of NaI(Tl) detectors, is dedicated to gamma-ray spectroscopy, offering high efficiency in detecting photons emitted from excited nuclear states. This capability is essential for nuclear structure studies. NEBULA, a neutron detection system, is optimized for time-of-flight measurements and can simultaneously detect multiple neutrons, enabling detailed studies of neutron-rich nuclei.

These detection systems has led to significant advancements in nuclear physics. Notable achievements include the discovery of new magic numbers [4, 5], the observation of a four-neutron resonance [6], and the first spectroscopy of isotopes near or beyond the drip line [7, 8]. These discoveries highlight the importance of continuous development in detection systems, improving sensitivity and addressing the challenges posed by higher beam intensities expected in future experiments.

At RIBF, stable primary beams are accelerated up to 345 MeV/u using a set of four cyclotrons. The last two accelerators and the following beam-lines are shown Fig. 1. These beams are used to generate radioactive isotopes by fragmentation or fission at the primary target located at the F0 focal plane. These processes are highly effective for producing a wide range of neutron-rich and proton-rich species, as they involve high-energy collisions that break nuclei apart or induce asymmetric splitting. The BigRIPS separator [9] selects and identifies isotopes of interest on an event-by-event basis. These isotopes are then directed to one of three magnetic spectrometers: ZeroDegree [9], SAMURAI [10], or SHARAQ [11].

MINOS has been used at the F8 focal plane in combination with ZeroDegree and at the F13 focal plane coupled with SAMURAI. At F8, the focus is on high-efficiency gamma-ray detection using the DALI2 and DALI2<sup>+</sup> [12] arrays surrounding MINOS. This setup allows for the determination of bound nuclear excitation energies and decay patterns, providing valuable insights into nuclear structure.

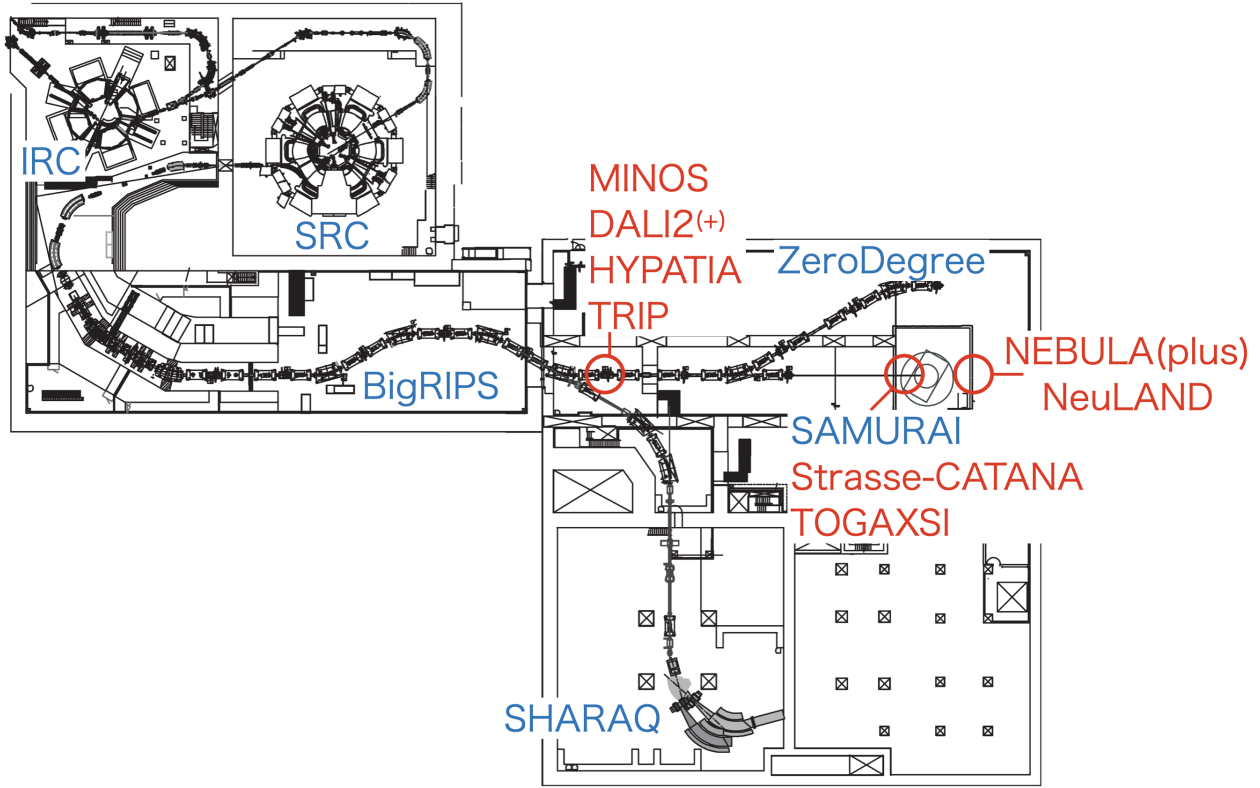


**Fig. 1** RIBF beamline, equipments and the location of detectors.

The SAMURAI spectrometer is primarily designed for invariant mass spectroscopy, a technique central to the study of exotic nuclei and their decay modes. While missing mass spectroscopy in inverse kinematics was not a primary focus at SAMURAI in the past, the spectrometer is now capable of combining both invariant mass and missing mass spectroscopy through the integration of new detection systems. This combination allows for a more comprehensive understanding of complex reaction processes and facilitates a detailed analysis of nuclear structure. Additionally, gamma-ray spectroscopy has been conducted at F13. This manuscript reviews the current detection devices at RIBF for nuclear reactions and discusses upcoming upgrades and developments. Section 2 focuses on developments related to the detection of charged light particles and clusters, Section 3 summarizes the gamma-ray arrays used at RIBF and their future plans, while Section 4 addresses the neutron detection systems.

## 2 Missing-mass spectroscopy in inverse kinematics

The RIBF produces RI beams with energies suitable for conducting quasi-free knock-out experiments. The advent of RIBF-stationed telescope arrays is essential for advancing missing-mass spectroscopy experiments. Although many physical interests have been explored, missing-mass spectroscopy using emitted particles from proton-induced knockout reactions could not be realized with the MINOS device due to its limited angular resolution.

Missing masses  $M_{miss}$  in inverse-kinematics proton-induced ( $p, pX$ ) knockout reactions are given by

$$M_{miss} = \sqrt{\{E_b + m_p - (E_p + E_X)\}^2 - \{\vec{P}_b - (\vec{P}_p + \vec{P}_X)\}^2}. \quad (1)$$

X represents the knocked-out particles, such as protons, deuterons, tritons,  $^3\text{He}$ , and  $\alpha$  particles.  $E_b$  and  $E_p$  denote the energy of the incoming beam and the recoil protons, respectively. The relation between kinematic energies and angles for the emitted particles in ( $p, pX$ ) reactions at incident energy of 200A MeV is shown in Fig. 2. It should be noted that, for simplicity, here the internal momentum of the X particle in the initial state was not taken into account. As shown in the left panel of Fig. 2, the masses of the knocked-out particles significantly affect the angular distributions, particularly the maximum angles in  $\theta_X$ . Ejectiles with mass numbers ranging from 2 to 4 appear at forward angles, smaller than 30 degrees. In contrast, the protons can be scattered up to 90 degrees.

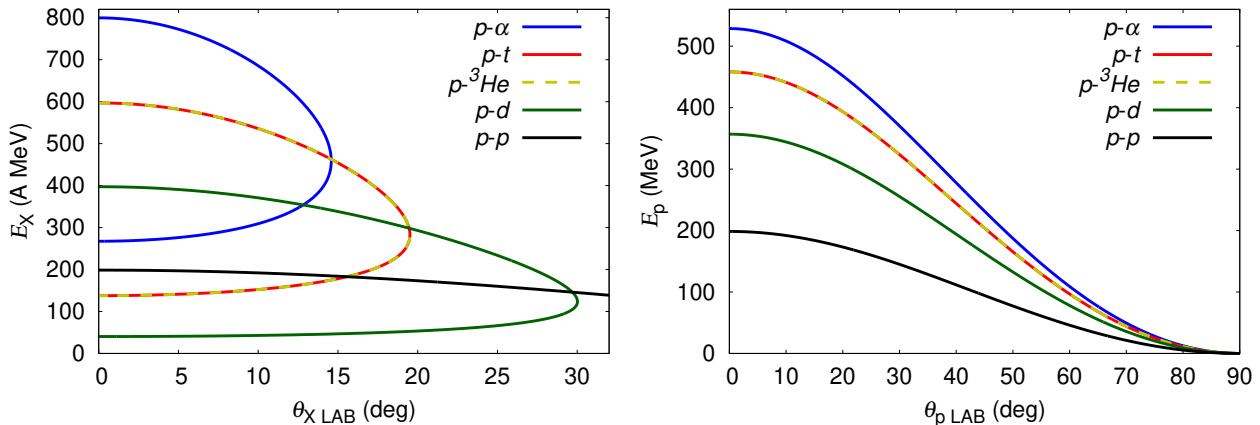


**Fig. 2** Relation between angles and energies of scattered particles X (left) and recoil protons (right) in inverse  $p - X$  scattering.

Quasi-free elastic scattering reactions can be described using relatively simple models. The nucleons in an atomic nucleus can be assumed to follow the Fermi gas model, which

treats the nucleus as a system with independent nucleons. The maximum wave number among the occupied states, the Fermi wave number, corresponds to the standard nuclear density of  $0.17 \text{ fm}^{-3}$ . This value translates to  $k = 1.36 \text{ fm}^{-1}$ , or approximately  $270 \text{ MeV}/c$  in the momentum space. When the momenta of the particles significantly exceed Fermi momentum due to reactions, the particles enter a quasi-free condition, no longer bound by the nuclear force. Achieving this condition requires incident beam energies to be sufficiently high. In inverse kinematics, the target proton gains momentum during the reaction, and that is nothing but the transferred momentum. Under the quasi-free approximation, the knocked-out particle is assumed to gain the same amount of momentum relative to the residual atomic nucleus, as illustrated in Fig. 3.

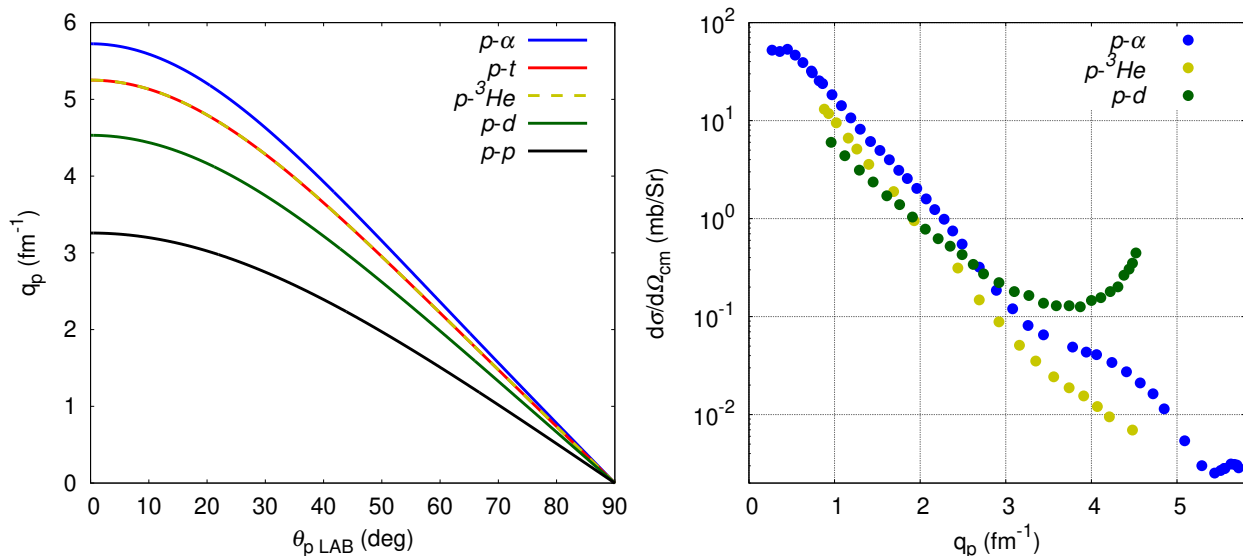


**Fig. 3** Left: Dependence of recoil proton momentum (wave-number) on laboratory angle. Right: Transfer momentum dependence of the differential cross section of  $p - X$  scattering at 200 MeV of incident protons [13–15]. (right).

As the transferred momentum increases, the impact parameter between protons and intra-nuclear particles before the knockout becomes smaller. Consequently, the quasi-free scattering cross-sections tend to decrease. The right panel of Fig. 3 illustrates the relationship between cross-sections and momentum transfers. When designing experimental devices and setups, it is essential to balance the acceptance of distributions after quasi-free scatterings with the need to maximize cross-sections to achieve realistic yields.

## 2.1 The telescope array for $(p, 2p)$ and $(p, 3p)$ reactions

The recoil protons are emitted at wide angles in the laboratory frame for the  $(p, 2p)$  and  $(p, 3p)$  reactions. STRASSE (Silicon Tracker for RAdioactive nuclei Studies at SAMURAI Experiments) [16] is a detection system under construction and optimized for  $(p, 2p)$  and  $(p, 3p)$  measurements at 200–250 MeV/nucleon at the RIBF facility. It consists of a compact silicon tracker placed in vacuum and a thick liquid hydrogen target with an effective diameter of 20 mm and a maximum length of 150 mm. STRASSE allows an optimum luminosity for beam intensities available at the RIBF. Thanks to the excellent reaction vertex resolution of 0.5 mm (FWHM), decent missing-mass spectra, which could not be achieved with the MINOS system, can be obtained with a resolution below 2 MeV. For  $(p, 2p)$  reactions at 250 MeV/nucleon, the one- and two-proton detection efficiencies of the silicon tracker are expected to be 86% and 49%, respectively. It is also designed to be used with large scintillator or germanium arrays.

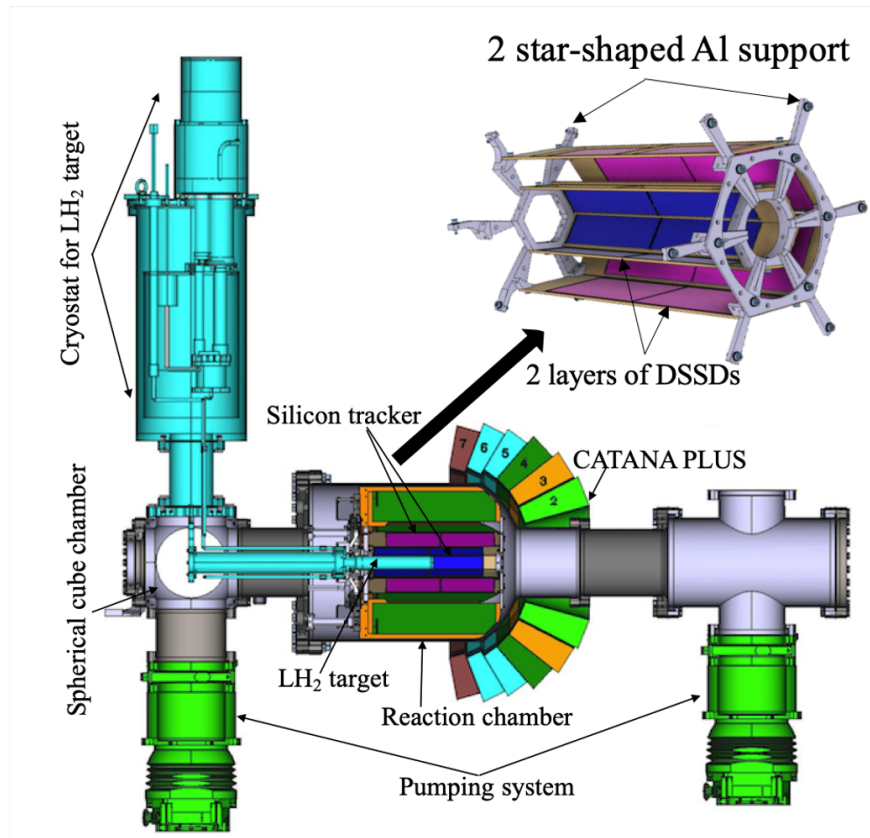


**Fig. 4** Schematic view of the overall conceptual design of the STRASSE detection system.

As shown in Fig. 4, the STRASSE silicon tracker is composed of two layers of double-sided silicon strip detectors (DSSDs) configured in a hexagonal shape. Each segment includes two DSSDs with strips parallel to the beam axis daisy chained. The inner segment has an active area of  $30 \text{ mm} \times 244 \text{ mm}$  with a thickness of  $200 \mu\text{m}$  and a pitch size of  $200 \mu\text{m}$ , while the outer segment has an active area of  $62.6 \text{ mm} \times 242 \text{ mm}$  with a thickness of  $300 \mu\text{m}$  and a pitch size of  $200 \mu\text{m}$ . The whole silicon tracker has a total of 17,358 electronic channels. 128-channel STS-XYTER [17] ASIC chips with the ability to detect minimum ionizing particles are used to read out the signals from DSSDs via custom-made low-mass and low-capacitance microcables. Each STS-XYTER has a 14-bit time stamp and a 5-bit flash ADC. They are wire-bonded to the front-end PCBs (FEBs) placed in the radial direction inside the vacuum chamber to achieve the required ENC  $\sim 10 \text{ keV}$ . A cooling system is designed to dissipate the heat load of the electronics. Two star-shaped stainless steel frames support the detectors. The data from different FEBs are then sent to a concentration board called GBTxEMU via a mezzanine connection board. A PCI-express GERI board receives the aggregated data via optical fibers and synchronizes different GBTxEMUs.

The geometry of the LH<sub>2</sub> target in STRASSE is designed to minimize the energy loss and angular straggling of the protons produced from quasi-free scattering. The target system consists of three parts: 1) the target cell made of  $175 \mu\text{m}$  Mylar foil with a 31-mm cylinder and a 20-mm entrance window, 2) the cryostat to liquefy the hydrogen at  $\sim 20 \text{ K}$ , and 3) the control command system and the gas circuit to ensure the safe operation of the target. The hydrogen circulation in the STRASSE target is driven by the thermal siphon as the former PRESPEC [18] and MINOS [3] targets. As shown in Fig. 4, two pumping stations located upstream and downstream of the STRASSE reaction chamber were used to achieve the required vacuum of the LH<sub>2</sub> target. STRASSE will be a standalone system with windows to isolate from the beamline pipes.

STRASSE will be mainly used together with the CATANA (Cesium iodide Array for  $\gamma$ -ray Transitions in Atomic Nuclei at high isospin Asymmetry) array [19]. It consists of CsI(Na) scintillators aligned at a radius of  $\sim 20 \text{ cm}$  to measure the energies of  $\gamma$  rays and recoil protons with the SAMURAI setup. After the upgrade, CATANA now has 160 CsI(Na) crystals arranged into 8 rings (L1-L8) covering the polar angle from 17 to 77 degrees. For crystals at L2 to L8, Hamamatsu R580 PMTs with modified circuits read out the signals from the anode for  $\gamma$  and the second last dynode for protons. Hamamatsu R11265 PMTs are used for crystals at L1. Note that the 40 Crystals at L1 and L2 are used only to detect protons. While for  $\gamma$ -ray detection, the energy resolution was measured to be 9% (FWHM) at 662 keV, for protons, the energy resolution was measured to be 1.7% (FWHM) using proton-proton elastic scattering at 230 MeV.

## 2.2 Elucidating cluster formation with $(p, pX)$ telescope

The particles released in knockout reactions are not necessarily to be protons and neutrons. By measuring cluster knockout reactions, it is possible to investigate the existence of clusters on the surface and inside of atomic nuclei. Alpha knockout reactions from stable tin isotopes, which is a stable nucleus, demonstrated the cluster formation in heavy nuclei [20]. Analyzing the emitted particles after the  $(p, p\alpha)$  reaction using a magnetic spectrometer, the cluster separation energy, a characteristic physical quantity of cluster knockout reaction, was deduced. It suggested that the isotopic dependence of cluster knockout reaction cross sections corresponds to the trend of alpha cluster formation predicted by theory. To extend the study towards the nuclei apart from the stability line, several inverse-kinematic alpha-knockout reactions in unstable nuclei experiments have been performed using solid and liquid hydrogen targets. In the following paragraphs, recent achievements of the particle spectroscopies performed in inverse kinematics are explained.

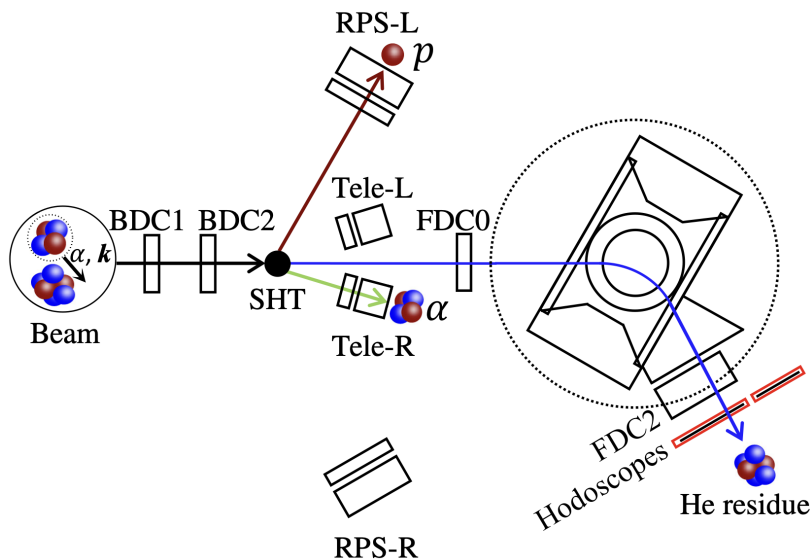


**Fig. 5** Experimental setup for  $^{10}\text{Be}(p, p\alpha)$  reaction experiment. The figure is taken from [21].

Figure 5 shows the experimental setup for measuring the alpha knockout reaction from a neutron-rich  $^{10}\text{Be}$  isotope. In this experiment, a 2-mm thick solid hydrogen target [22] was used. The surrounding detectors were placed far away so that the opening angle of the target thickness seen from the detector becomes small resulting in the alpha separation energy resolution of 1.06 MeV in sigma. As the emitted particles, protons, and alpha particles differ



significantly in emission angle and energy, different detectors were placed at the respective emission angles. The recoil proton spectrometer (RPS-L(R)) [23, 24] consisting of a drift chamber and a NaI (Tl) scintillator was prepared for the detection of the protons at 60 degrees from the beam axis. A silicon detector and CsI (Tl) telescope (Tele-L(R)) [25] was prepared for the alpha particles in forward angles of 4-12 degrees. Furthermore, the  ${}^6\text{He}$  residues were analyzed by the SAMURAI spectrometer installed forward. As a result, the triple differential cross section concerning the energy of protons suggested an alpha cluster structure mediating the two alphas + two neutrons picture of  ${}^{10}\text{Be}$ .

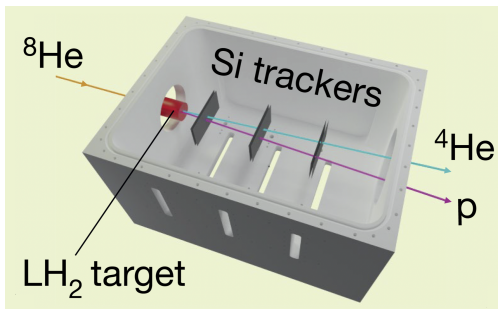


**Fig. 6** Silicon trackers for  ${}^8\text{He}(p, p\alpha)$  reaction experiment. The figure is taken from [6].

The alpha knockout reaction can also be used to reach uninvestigated nuclear systems. Here, the detection apparatus employed in the experiment for tetra-neutron search via  ${}^8\text{He}(p, p\alpha)$  is introduced. As described in Fig. 6, silicon-strip detectors were placed downstream of the 50-mm-thick MINOS liquid hydrogen target. The detector arrangement was specialized for such events that alpha clusters in  ${}^8\text{He}$  nuclei collide with protons with small impact factors. The forward ejected protons and trailing alpha particles were tracked with three layers of strip silicon detectors, and their momenta were analyzed with the SAMURAI spectrometer.

In both cases described above, missing mass energy resolutions have been achieved as low as 1 MeV, however, the limitations in the solid angles are necessary to be improved. It will be crucial for the next-generation devices to inherit the successful concept of MINOS, thick target, and large solid angle, compensating for the weak RI beam intensity and achieving high detection efficiency. In addition, it would be ideal to measure multiple types of cluster knockout reactions over wide solid angles with one configuration. Incorporating a total energy calorimeter for the emitted particles can ensure the missing mass spectroscopy. Should the quasi-free scattering condition hold in inverse kinematics, these particles will be emitted at high energies towards relatively forward angles, while the recoil protons will be ejected to

larger angles. The residues move forward along the beam axis. The detector array introduced in the following paragraph is designed to measure these charged particles at once, providing almost 1 MeV ( $\sigma$ ) missing mass energy resolution.

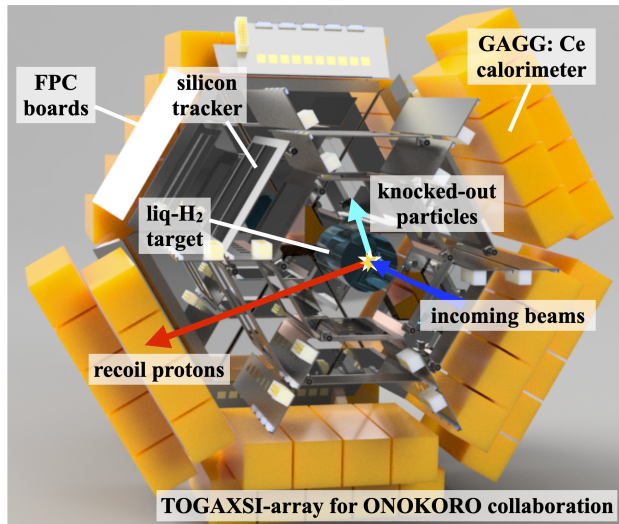


**Fig. 7** Graphical design of TOGAXSI array.

Figure 7 shows the TOGAXSI (TOtal energy measurement by GAgg and verteX measurement by Silicon strips) telescope [26] being developed in the cluster knockout reaction project “ONOKORO” [27]. It consists of telescope modules with a silicon tracker and a GAGG(Ce) calorimeter for each. Development is reduced by adapting the same type of liquid hydrogen target as the STRASSE [16]. A quasi-free scattering condition imposes criteria of momentum transfer of  $2 \text{ fm}^{-1}$  and more. Here we assume experiments with 200A MeV incoming beams, which kinematics are shown in Fig. 2. The momentum transfer and its trend of cross sections are shown in Fig. 3. From the momentum transfer of  $2 \text{ fm}^{-1}$ , on the higher momentum side, the detector should cover at which the differential cross section is  $1/10$  to keep the realistic yields. In the right panel of Fig. 3, it is almost  $3 \text{ fm}^{-1}$ . Based on the condition, the protons are designed to cover a polar angle of 8 to 30 degrees, and the cluster particles cover a polar angle of 35 to 70 degrees, respectively. The silicon tracker consists of three layers of silicon-strip detectors with a thickness of  $100 \mu\text{m}$  and a pitch of  $100 \mu\text{m}$ . It is assumed to satisfy the required 3 mrad tracking resolution [28]. In the condition above the proton energy varies from 80-250 MeV, and the cluster particle energy is 75-180A MeV in the covered angles (Please see the relation of energy and angle in Fig. 2). GAGG(Ce) has been adopted as the material of the calorimeter. This is because of its high stopping power against

charged particles due to its high density of  $6.63 \text{ g/cm}^3$  and the high energy resolution in a non-deliquescent scintillation crystal. Relatively large crystals of  $35 \text{ mm} \times 35 \text{ mm} \times 120 \text{ mm}$  were chosen so that to stop high-energy charged particles. The construction of the full array is underway. The TOGAXSI is expected to accelerate comprehensive cluster research with missing mass spectroscopy based on the detection of charged particles.

### 3 Gamma-ray detection for gamma-ray spectroscopy

In-beam  $\gamma$ -ray spectroscopy is a powerful tool that allows the study of nuclear structure and excited states of atomic nuclei. The advent of RIBs has increased the potential of this technique as new mass regions can be explored and new phenomena can be observed. Indeed, high primary beam intensities have enabled the production of short-lived isotopes which in turn can impinge on solid or liquid targets to induce Coulomb excitation, inelastic scattering, knockout, and two-step fragmentation experiments in inverse kinematics [29].

At the RIBF, secondary beams with incident energies of 100 to 250 MeV/ $u$  are used to populate excited states of nuclei far from stability. While such energies allow the use of thicker targets, and therefore increase the luminosity, they also present different experimental challenges. Of particular importance are the large Doppler shift of the detected  $\gamma$ -rays, and the background generated by either atomic or nuclear processes.

Observed  $\gamma$ -ray energies,  $E_\gamma$ , are Doppler shifted with respect to the emitted energies in the rest frame,  $E_{\gamma 0}$ , following the relation

$$\frac{E_{\gamma 0}}{E_\gamma} = \frac{1 - \beta \cos \theta_\gamma}{\sqrt{1 - \beta^2}}, \quad (2)$$

where  $\beta$  denotes the velocity of the beam and  $\theta_\gamma$  is the angle between the particle direction and the  $\gamma$ -ray emission in the laboratory frame of reference. The energy resolution that can be achieved is therefore limited by the uncertainties in the velocity,  $\Delta\beta$ , the emission angle of the  $\gamma$ -ray,  $\Delta\theta_\gamma$ , and the intrinsic resolution of the detection material,  $\Delta E_\gamma$ . In general, the use of thicker secondary targets leads to a higher energy loss and therefore a larger contribution to  $\Delta\beta$ . The use of MINOS [3] overcomes this problem by tracking the protons ejected from the target after knockout reactions and reconstructing the interaction position. In this way thicker targets can be used without affecting the achievable energy resolution as shown in Fig. 8. While the intrinsic resolution,  $\Delta E_\gamma$ , is a property of the detector material, the angular resolution,  $\Delta\theta_\gamma$ , can be improved either by reducing the size of the detectors or by implementing a position-sensitive readout with a sub-centimeter resolution for the first interaction of the  $\gamma$ -rays. Figure 8 shows the effect of using the HYPATIA array (described below), which has a better intrinsic resolution than DALI2 [1, 12], as well as smaller detectors.

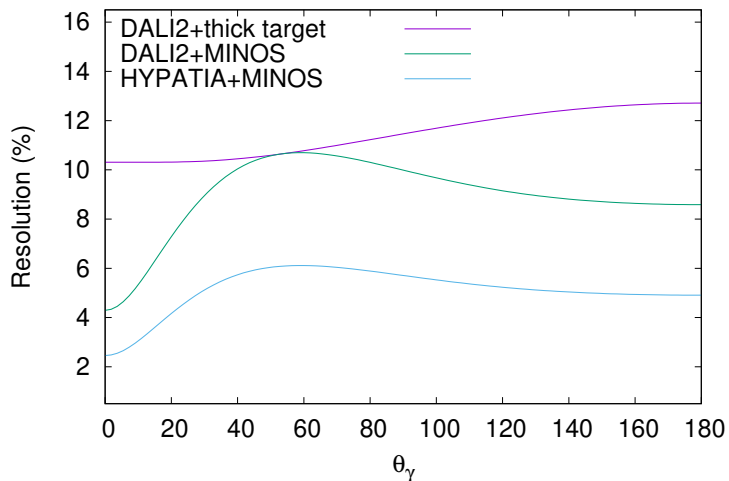


**Fig. 8** Total energy resolution for different  $\gamma$ -ray spectrometers. For a thick target, a large  $\Delta\beta$  is obtained. This uncertainty is reduced by using MINOS. The use of smaller detectors with better intrinsic resolution, as the HYPATIA array, further improve the achievable energy resolution. The calculations were performed for  $\beta = 0.6$  and a 1 MeV  $\gamma$ -ray energy assuming a square-root dependence of the intrinsic energy resolution

In addition to the energy resolution, the total efficiency of the detection array is an important factor. The use of high-efficiency materials becomes critical for the study of nuclei at the limit of existence where few events are expected, and for reconstructing complicated level schemes with multiple  $\gamma$ -ray emissions. In general,  $\gamma$ -ray detection arrays can be optimized either for an increased energy resolution or for a high detection efficiency.

A further parameter to be considered is the time resolution. The high background generated in these type of experiments is usually a limiting factor, specially at low energies. It can be reduced by selecting events correlated to the impinging particle within a short time window. The successful use of this technique requires a time resolution typically better than 1 ns. Such resolution is only achievable for some scintillation materials.

The interplay of different factors makes it necessary to tackle the next generation  $\gamma$ -ray arrays from different perspectives, which depend on the physics cases pursued. In the following, we make a summary of future projects regarding  $\gamma$ -ray detection arrays at the RIBF.

### 3.1 Towards a new scintillation detector array: The HYPATIA project

Since 2001 the main device used at the RIBF to perform in-beam  $\gamma$ -ray spectroscopy has been the DALI2 array [1], composed of 186 NaI(Tl) detectors. From 2017 the upgraded

DALI2<sup>+</sup> array [12], consisting of 226 NaI(Tl) detectors, covering a large solid angle and offering a high detection efficiency, has been employed to detect radiation emitted primarily after direct reactions with RIBs.

Significant results have been obtained using the DALI2 and DALI2<sup>+</sup> array, notably the discovery of a new magic number at  $N = 34$  [4], the spectroscopy of first excited states in the “Island of Inversion” [30, 31], and the first spectroscopy of the most exotic neutron-rich isotopes accessible to date within the SEASTAR project [32]. Given the future upgrade of the RIBF [33], a new  $\gamma$ -ray detection array is required to fully exploit the new experimental capabilities that come along with it.

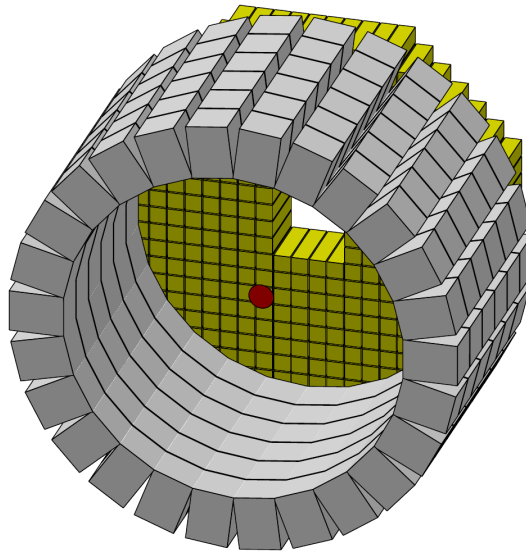


**Fig. 9** Conceptual design of the HYPATIA array composed of a barrel of CeBr<sub>3</sub> detectors and a forward wall of HR-GAGG crystals.

Based on the experience acquired during the last two decades using DALI2 and DALI2<sup>+</sup>, the key characteristics desired for this new array are:

- Higher detection efficiency which would allow to reach more exotic isotopes, as well as to perform detailed  $\gamma - \gamma$  coincidences analysis to build level schemes.
- Better energy resolution to identify previously unresolved transitions and exploit lifetime effects.
- Improved time resolution to suppress the beam-related background.
- A versatile design which allows to install of the array at different locations and with varying configurations optimized for each measurement.

With this requirement in mind, the HYPATIA (HYbrid Photon detector Array To Investigate Atomic nuclei) array has been designed [34]. This array, depicted in Fig. 9, consists of 624 Cerium Bromide ( $\text{CeBr}_3$ ) detectors of  $30 \times 30 \times 80 \text{ mm}^2$  forming a barrel around the target and 384 Cerium-doped Gadolinium Aluminum Gallium Garnet (HR-GAGG) detectors of  $25 \times 25 \times 100 \text{ mm}^2$  placed as a forward wall. The  $\text{CeBr}_3$  detectors were chosen due to their improved energy- and time-resolution compared to  $\text{NaI}(\text{Tl})$ , their reasonable cost, and the lack of intrinsic radiation. On the other hand, the HR-GAGG crystals are non-hygroscopic and have a high effective atomic number, therefore offering the possibility to minimize the dead space and increase the efficiency and peak-to-total ratio at forward angles. Thanks to the cuboidal shape of all the detectors, it is possible to arrange them in different configurations, including surrounding the MINOS or STRASSE targets, as well as to place the array at the different spectrometers of the RIBF. Furthermore, the selected shapes and sizes of the detectors are compatible with the mechanical structure of the DALI2<sup>+</sup> array, therefore it will be possible to gradually replace the detectors without interrupting the physics program.

The future availability of  $^{238}\text{U}$  primary beam at 345 MeV/nucleon with an intensity of 2000 pnA would allow the production of very exotic isotopes towards the drip lines. Inelastic scattering, Coulomb excitation, transfer reaction, and quasi-free scattering reactions can be employed to study these isotopes. Thanks to its superior efficiency, time resolution, and peak-to-total ratio, the HYPATIA array will be able to overcome some of the limitations of DALI2<sup>+</sup>, as well as of high-resolution Ge detectors which do not cover a solid angle of  $4\pi$ , such as the pandemonium effect. A key example of the possibilities of HYPATIA with the fast beam at the RIBF is the first spectroscopy of  $^{60}\text{Ca}$ .

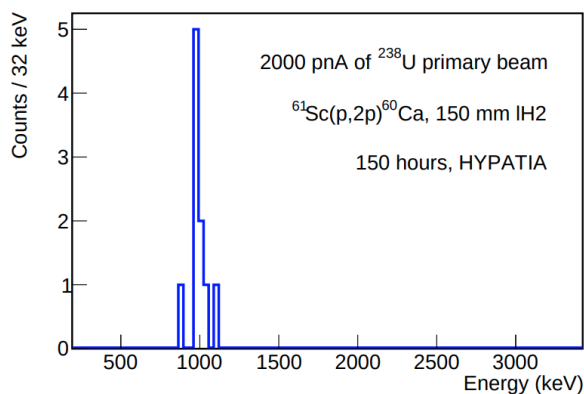


**Fig. 10** Expected Doppler-corrected  $\gamma$  spectrum of  $^{60}\text{Ca}$  for a 150-hour measurement with HYPATIA.

The Ca isotopic chain is particularly interesting for nuclear structure studies. While the proton shell closure at  $Z = 20$  seems to be maintained, new neutron shell closures at  $N = 32$  and  $N = 34$  have been evidenced by spectroscopy [4, 35], mass measurements [36, 37], and knockout reaction cross sections [38, 39]. The possibility of a further magic number at the  $N = 40$  harmonic-oscillator shell closure has been widely studied [40, 41]. Although measurements on  $^{58}\text{Ca}$  [42] and  $^{62}\text{Ti}$  [43], the closest neighbours of  $^{60}\text{Ca}$ , show no indication of a shell closure at  $N = 40$ , only the first spectroscopy of  $^{60}\text{Ca}$  can provide definitive answers. This measurement will be possible with the HYPATIA array, as shown in Fig. 10, where the simulated  $\gamma$ -ray spectrum obtained in a 150 h measurement is shown.

### *3.2 Future projects with Ge detectors*

The  $\gamma$ -ray tracking technique of Ge detectors is the state-of-the-art method to achieve the best energy resolution for  $\gamma$ -rays. This technique has been implemented in the latest large-scale Ge arrays GRETINA [44] and AGATA [45]. During 2020 and 2021, the RIBF hosted the HiCARI array [46] to conduct the first studies with tracking-type germanium detectors, which yielded successful outcomes. HiCARI was organized as a one-time campaign of experiments at the RIBF by gathering Ge detectors from other facilities. It is desirable to make continued efforts to push in-beam  $\gamma$ -ray spectroscopy based on tracking technology forward. For this reason, the Gamma-ray Tracking in R5 (GT-5) project was launched in 2023 at the RIKEN Nishina Center as a common and long-term platform for tracking-type Ge detectors at the RIBF to drive physics experiments and instrumentation for tracking technologies. The GT-5 has its own scientific and development programs related to in-beam  $\gamma$ -ray spectroscopy using RIBs. On a hardware basis, the GT-5 presently encompasses two in-house tracking detectors. One is the Compton camera telescope GREI [47], and the other is a position-sensitive strip germanium telescope SGT [48], both based on planar crystals with stripped segments. Furthermore, a GRETINA quad-type module was procured in 2023. In addition to the detectors, a maintenance facility for Ge detectors, electronics, and infrastructure is arranged. A unique aspect of the GT-5 is that it is not only involved in the scientific activities of the RIBF but also the framework of the TRIP (Transformative Research Innovation Platform of RIKEN platforms) project, a RIKEN-wide initiative starting in 2023. One of the main goals of the TRIP use case is to establish an optical model for radioactive isotopes that are needed for reaction analyses and predictions but have yet to be studied based on systematic experimental data. To provide systematic data to optimize optical model potential parameters, the GT-5 is teamed with the elastic scattering measurement program MESA (Measurement of Elastic Scattering Anytime anywhere on any beam) and the reaction

cross-section measurement program S3CAN (Symbiotic Systematic and Simultaneous Cross-section measurements for All over the Nuclear chart). As the first opportunities for data collection, experiments with stable beams at the RIPS and with RIBs of the BigRIPS will be conducted in 2024.

## 4 Neutron detection for invariant-mass spectroscopy

Invariant mass spectroscopy is a powerful tool for measuring the properties of nuclei under extreme isospin conditions. In particular, for neutron-rich isotopes, phenomena such as halo structures near the neutron drip line, neutron correlations, unbound states, and new cluster states are to be expected. The study of such properties allows us not only to probe the mechanisms underlying the nuclear force but also to better understand the nuclear equation of state and to investigate the properties of neutron stars. Such neutron-rich systems can be produced using different types of reactions with radioactive beams, and their structure can be determined by measuring the momenta of all the outgoing particles, including neutrons, following the decay of any intermediate resonance.

Kinematically complete measurements are performed at the SAMURAI spectrometer of the RIBF. For the detection of the fast neutrons evaporated after the reactions, the NEBULA (NEutron detection system for Breakup of Unstable nuclei with Large Acceptance) detector has been employed [2]. NEBULA is made up of two identical wall structures, which consist of a layer of VETO scintillation detectors to eliminate hits from charged particles and two-layered neutron detectors with 30 each scintillation bars with readouts by PMTs at both ends. Each neutron detection bar is shaped as  $12 \times 12 \times 180 \text{ cm}^3$ , featuring high neutron detection efficiency, large angular coverage, and capability of multiple neutron coincidence detection. A further improvement in the multiple neutron detection efficiency was achieved by combining NEBULA with NeuLAND (New Large-Area Neutron Detector), a new neutron detector array developed for the R3B setup under construction at FAIR [49]. With this combined setup, a diversity of phenomena has been measured, such as the first measurement of  $^{28}\text{O}$  [8].

The upgrade plans of the RIBF will enable to reach of further neutron-rich isotopes, which are expected to have various weakly bound multi-neutron systems. To extend the sensitivity of multi-neutron reconstructions, a project to extend the detector volume for better detection efficiency, NEBULA Plus, is in progress through a collaborative effort between Japan and LPC Caen in France, as part of the French-funded EXPAND project [50]. The NEBULA Plus array consisting of 90 new modules has been integrated with the existing



array, effectively doubling the number of detection layers. This expansion increases the one-neutron detection efficiency by nearly a factor of 2 and improve the four-neutron detection efficiency by almost one order of magnitude. Initial in-beam tests are scheduled at the RIBF in the near future [51]. Physics opportunities such as the investigation of the two-neutron decay of  $^{21}\text{B}$ , the search for  $^{21}\text{B}^*$ , and the measurement of a three-neutron decay of  $^{20}\text{B}$ , are expected to be accessible with the NEBULA Plus detector.

In contrast, a detector focused on more precise measurement by improving the achievable resolution in measurements of neutron momentum is also being constructed. The High-resolution Detector Array for Multi-neutron Events (HIME) detector was originally developed by the group of The Tokyo Institute of Technology (now Institute of Science Tokyo), and further collaborated with the Technical University of Darmstadt. The optimized energy resolution of HIME is achieved through the use of smaller scintillator bars with dimensions of  $4 \times 2 \times 100 \text{ cm}^3$ , which improves position resolution, and new electronics for a higher time precision. It consists of layers of scintillator bars arranged in both the  $x$  and  $y$  directions alternatively [52]. This arrangement will not only improve its resolution, but will also allow discriminating the hits due to recoiling protons, allowing the selection of valid events and reducing cross-talk [53]. Currently, a prototype of HIME has been built, and more layers are in construction at TU Darmstadt. The improved energy resolution will enable precise measurements, such as the neutron-neutron scattering length, which characterizes the two-neutron interactions at low energies. Besides that, it is considered to be used for the detection of the recoil neutrons after the  $(p, pn)$  reactions in combination with the proton trackers as described in the previous sections.

## 5 Conclusion

In conclusion, detector research and development (R&D) plays a crucial role in acquiring new physical data on quasi-free scattering using unstable nuclei. This review highlights several detectors that are either planned or under construction. One of the key projects is the STRASSE detection system, which is optimized for high-energy proton reactions and is under construction at the RIBF facility. It consists of a compact silicon tracker and a thick liquid hydrogen target, enabling high-resolution measurements of missing mass in proton-induced reactions. The system is designed to work in conjunction with the CATANA array, enhancing the detection of gamma rays and recoil protons with excellent energy resolution.

Another key project is the TOGAXSI telescope, developed as part of the ONOKORO project. It is designed to meet strict requirements for momentum transfer and angular coverage. With its advanced silicon trackers and GAGG(Ce) calorimeters, TOGAXSI is expected to significantly advance cluster research through high-precision missing mass spectroscopy.

In addition, in-beam  $\gamma$ -ray spectroscopy has proven essential for studying nuclear structure and excited states. The RIBF facility uses the DALI2 and its upgraded DALI2<sup>+</sup> arrays to make groundbreaking discoveries, such as identifying the magic number at  $N = 34$  and exploring the "Island of Inversion." To fully benefit from upcoming RIBF upgrades, the next-generation HYPATIA array has been designed. It combines high-efficiency CeBr<sub>3</sub> and HR-GAGG detectors in a modular, versatile configuration. This will provide better resolution, greater efficiency, and reduced background, ensuring continued progress in exploring exotic nuclei and their properties far from stability. Additionally, the future availability of a <sup>238</sup>U primary beam at 345 MeV/nucleon with an intensity of 2000 pnA will enable the production of very exotic isotopes towards the drip lines. With its superior efficiency, time resolution, and peak-to-total ratio, the HYPATIA array will overcome previous limitations and make possible the first spectroscopy of <sup>60</sup>Ca, along with other critical measurements for nuclear structure studies.

Furthermore, the state-of-the-art  $\gamma$ -ray tracking technique using Ge detectors has achieved significant breakthroughs in energy resolution. This is demonstrated by large-scale arrays such as GRETINA and AGATA. The GT-5 project, launched in 2023, aims to push the boundaries of in-beam  $\gamma$ -ray spectroscopy by integrating advanced tracking technology. It will provide systematic data to optimize optical models and enhance reaction analysis through collaborations with programs such as MESA and S3CAN.

Invariant mass spectroscopy is also proving to be an invaluable tool for understanding neutron-rich isotopes. The SAMURAI spectrometer and NEBULA detector are enabling the study of phenomena such as halo structures and unbound states. The development of NEBULA Plus and HIME will further improve neutron detection efficiency and energy resolution. This will open up new opportunities for precise measurements, such as the neutron-neutron scattering length, and advance our understanding of nuclear structure and neutron star properties.

## Acknowledgment

The authors acknowledge the contributions of Tomohiro Uesaka, Nigel Orr, Yasuhiro Togano, Marco Knösel, Valerii Panin, Ryotaro Tsuji, Rin Yokoyama, Pieter Doornenbal, Marina Petri, and Daisuke Suzuki. J.T. also acknowledges the ONOKORO collaboration.

## References

- [1] S Takeuchi, T Motobayashi, Y Togano, M Matsushita, N Aoi, K Demichi, H Hasegawa, and H Murakami, Nuclear Instruments and Methods in Physics Research Section A: Accelerators, Spectrometers, Detectors and Associated Equipment, **763**, 596–603 (2014).
- [2] Y. Kondo, T. Tomai, and T. Nakamura, Nuclear Instruments and Methods in Physics Research Section B: Beam Interactions with Materials and Atoms, **463**, 173–178 (2020).
- [3] A. Obertelli, A. Delbart, S. Anvar, L. Audirac, G. Authelet, H. Baba, B. Bruyneel, D. Calvet, F. Château, A. Corsi, P. Doornenbal, J.-M. Gheller, A. Giganon, C. Lahonde-Hamdoun, D. Leboeuf, D. Loiseau, A. Mohamed, J. Ph. Mols, H. Otsu, C. Péron, A. Peyaud, E. C. Pollacco, G. Prono, J.-Y. Rousse, C. Santamaria, and T. Uesaka, The European Physical Journal A, **50**(1), 8 (Jan 2014).
- [4] D. Steppenbeck, S. Takeuchi, N. Aoi, P. Doornenbal, M. Matsushita, H. Wang, H. Baba, N. Fukuda, S. Go, M. Honma, J. Lee, K. Matsui, S. Michimasa, T. Motobayashi, D. Nishimura, T. Otsuka, H. Sakurai, Y. Shiga, P.-A. Söderström, T. Sumikama, H. Suzuki, R. Taniuchi, Y. Utsuno, J. J. Valiente-Dobón, and K. Yoneda, Nature, **502**(7470), 207–210 (Oct 2013).
- [5] R. Taniuchi, C. Santamaria, P. Doornenbal, A. Obertelli, K. Yoneda, G. Authelet, H. Baba, D. Calvet, F. Château, A. Corsi, A. Delbart, J.-M. Gheller, A. Gillibert, J. D. Holt, T. Isobe, V. Lapoux, M. Matsushita, J. Menéndez, S. Momiyama, T. Motobayashi, M. Niikura, F. Nowacki, K. Ogata, H. Otsu, T. Otsuka, C. Péron, S. Péru, A. Peyaud, E. C. Pollacco, A. Poves, J.-Y. Roussé, H. Sakurai, A. Schwenk, Y. Shiga, J. Simonis, S. R. Stroberg, S. Takeuchi, Y. Tsunoda, T. Uesaka, H. Wang, F. Browne, L. X. Chung, Z. Dombradi, S. Franco, F. Giacoppo, A. Gottardo, K. Hadynska-Klek, Z. Korkulu, S. Koyama, Y. Kubota, J. Lee, M. Lettmann, C. Louchart, R. Lozeva, K. Matsui, T. Miyazaki, S. Nishimura, L. Olivier, S. Ota, Z. Patel, E. Şahin, C. Shand, P.-A. Söderström, I. Stefan, D. Steppenbeck, T. Sumikama, D. Suzuki, Z. Vajta, V. Werner, J. Wu, and Z. Y. Xu, Nature, **569**(7754), 53–58 (May 2019).
- [6] M. Duer, T. Aumann, R. Gernhäuser, V. Panin, S. Paschalis, D. M. Rossi, N. L. Achouri, D. Ahn, H. Baba, C. A. Bertulani, M. Böhmer, K. Boretzky, C. Caesar, N. Chiga, A. Corsi, D. Cortina-Gil, C. A. Douma, F. Dufter, Z. Elekes, J. Feng, B. Fernández-Domínguez, U. Forsberg, N. Fukuda, I. Gasparic, Z. Ge, J. M. Gheller, J. Gibelin, A. Gillibert, K. I. Hahn, Z. Halász, M. N. Harakeh, A. Hirayama, M. Holl, N. Inabe, T. Isobe, J. Kahlbow, N. Kalantar-Nayestanaki, D. Kim, S. Kim, T. Kobayashi, Y. Kondo, D. Körper, P. Koseoglou, Y. Kubota, I. Kuti, P. J. Li, C. Lehr, S. Lindberg, Y. Liu, F. M. Marqués, S. Masuoka, M. Matsumoto, J. Mayer, K. Miki, B. Monteagudo, T. Nakamura, T. Nilsson, A. Obertelli, N. A. Orr, H. Otsu, S. Y. Park, M. Parlog, P. M. Potlog, S. Reichert, A. Revel, A. T. Saito, M. Sasano, H. Scheit, F. Schindler, S. Shimoura, H. Simon, L. Stuhl, H. Suzuki, D. Symochko, H. Takeda, J. Tanaka, Y. Togano, T. Tomai, H. T. Törnqvist, J. Tscheuschner, T. Uesaka, V. Wagner, H. Yamada, B. Yang, L. Yang, Z. H. Yang, M. Yasuda, K. Yoneda, L. Zanetti, J. Zenihiro, and M. V. Zhukov, Nature, **606**(7915), 678–682 (Jun 2022).
- [7] H. L. Crawford, P. Fallon, A. O. Macchiavelli, P. Doornenbal, N. Aoi, F. Browne, C. M. Campbell, S. Chen, R. M. Clark, M. L. Cortés, M. Cromaz, E. Ideguchi, M. D. Jones, R. Kanungo, M. MacCormick, S. Momiyama, I. Murray, M. Niikura, S. Paschalis, M. Petri, H. Sakurai, M. Salathe, P. Schrock, D. Steppenbeck, S. Takeuchi, Y. K. Tanaka, R. Taniuchi, H. Wang, and K. Wimmer, Phys. Rev. Lett., **122**, 052501 (Feb 2019).
- [8] Y. Kondo, N. L. Achouri, H. Al Falou, L. Atar, T. Aumann, H. Baba, K. Boretzky, C. Caesar, D. Calvet, H. Chae, N. Chiga, A. Corsi, F. Delaunay, A. Delbart, Q. Deshayes, Zs. Dombrádi, C. A. Douma, A. Ekström, Z. Elekes, C. Forssén, I. Gašparić, J.-M. Gheller, J. Gibelin, A. Gillibert, G. Hagen, M. N. Harakeh, A. Hirayama, C. R. Hoffman, M. Holl, A. Horvat, Á. Horváth, J. W. Hwang, T. Isobe, W. G. Jiang, J. Kahlbow, N. Kalantar-Nayestanaki, S. Kawase, S. Kim, K. Kisamori, T. Kobayashi, D. Körper, S. Koyama, I. Kuti, V. Lapoux, S. Lindberg, F. M. Marqués, S. Masuoka, J. Mayer, K. Miki, T. Murakami, M. Najafi, T. Nakamura, K. Nakano, N. Nakatsuka, T. Nilsson, A. Obertelli, K. Ogata, F. de Oliveira Santos, N. A. Orr, H. Otsu, T. Otsuka, T. Ozaki, V. Panin, T. Papenbrock, S. Paschalis, A. Revel, D. Rossi, A. T. Saito, T. Y. Saito, M. Sasano, H. Sato, Y. Satou, H. Scheit, F. Schindler, P. Schrock, M. Shikata, N. Shimizu, Y. Shimizu, H. Simon, D. Sohler, O. Sorlin, L. Stuhl, Z. H. Sun, S. Takeuchi, M. Tanaka, M. Thoennessen, H. Törnqvist, Y. Togano, T. Tomai, J. Tscheuschner, J. Tsubota, N. Tsunoda, T. Uesaka, Y. Utsuno, I. Vernon, H. Wang, Z. Yang, M. Yasuda, K. Yoneda, and S. Yoshida, Nature, **620**(7976), 965–970 (Aug 2023).
- [9] Toshiyuki Kubo, Daisuke Kameda, Hiroshi Suzuki, Naoki Fukuda, Hiroyuki Takeda, Yoshiyuki Yanagisawa, Masao Ohtake, Kensuke Kusaka, Koichi Yoshida, Naohito Inabe, Tetsuya Ohnishi, Atsushi Yoshida, Kanenobu Tanaka, and Yutaka Mizoi, Progress of Theoretical and Experimental Physics, **2012**(1), 03C003 (12 2012), <https://academic.oup.com/ptep/article-pdf/2012/1/03C003/11595011/pts064.pdf>.
- [10] T. Kobayashi, N. Chiga, T. Isobe, Y. Kondo, T. Kubo, K. Kusaka, T. Motobayashi, T. Nakamura, J. Ohnishi, H. Okuno, H. Otsu, T. Sako, H. Sato, Y. Shimizu, K. Sekiguchi, K. Takahashi, R. Tanaka, and K. Yoneda, Nuclear Instruments and Methods in Physics Research Section B: Beam Interactions with Materials and Atoms,

- 317**, 294–304, XVIth International Conference on ElectroMagnetic Isotope Separators and Techniques Related to their Applications, December 2–7, 2012 at Matsue, Japan (2013).
- [11] T. Uesaka, S. Shimoura, H. Sakai, G.P.A. Berg, K. Nakanishi, Y. Sasamoto, A. Saito, S. Michimasa, T. Kawabata, and T. Kubo, *Nuclear Instruments and Methods in Physics Research Section B: Beam Interactions with Materials and Atoms*, **266**(19), 4218–4222, Proceedings of the XVth International Conference on Electromagnetic Isotope Separators and Techniques Related to their Applications (2008).
- [12] I. Murray et al., *RIKEN Accel. Prog. Rep.*, **51**, 158 (2017).
- [13] K Ermisch, HR Amir-Ahmadi, AM Van Den Berg, R Castelijn, B Davids, A Deltuva, E Epelbaum, W Glöckle, Jacek Golak, MN Harakeh, et al., *Physical Review C*, **71**(6), 064004 (2005).
- [14] DK Hasell, A Bracco, HP Gubler, WP Lee, WTH van Oers, R Abegg, DA Hutcheon, CA Miller, JM Cameron, LG Greeniaus, et al., *Physical Review C*, **34**(1), 236 (1986).
- [15] GA Moss, LG Greeniaus, JM Cameron, DA Hutcheon, RL Liljestrand, CA Miller, G Roy, BKS Koene, WTH Van Oers, AW Stetz, et al., *Physical Review C*, **21**(5), 1932 (1980).
- [16] H. N. Liu, F. Flavigny, H. Baba, M. Boehmer, U. Bonnes, V. Borshchov, P. Doornenbal, N. Ebina, M. Enciu, A. Frotscher, R. Gernhäuser, V. Girard-Alcindor, D. Goupillière, J. Heuser, R. Kapell, Y. Kondo, H. Lee, J. Lehnert, T. Matsui, A. Matta, T. Nakamura, A. Obertelli, T. Pohl, M. Protsenko, M. Sasano, Y. Satou, C. J. Schmidt, K. Schünemann, C. Simons, Y. L. Sun, J. Tanaka, Y. Togano, T. Tomai, I. Tymchuk, T. Uesaka, R. Visinka, H. Wang, and F. Wienholtz, *The European Physical Journal A*, **59**(6), 121 (2023).
- [17] K. Kasinski, A. Rodriguez-Rodriguez, J. Lehnert, W. Zubrzycka, R. Szczygiel, P. Otfinowski, R. Kleczek, and C.J. Schmidt, *Nuclear Instruments and Methods in Physics Research Section A: Accelerators, Spectrometers, Detectors and Associated Equipment*, **908**, 225–235 (2018).
- [18] C. Louchart, J.M. Gheller, Ph. Chesny, G. Authelet, J.Y. Rouse, A. Obertelli, P. Boutachkov, S. Pietri, F. Ameil, L. Audirac, A. Corsi, Z. Dombardi, J. Gerl, A. Gillibert, W. Korten, C. Mailleret, E. Merchan, C. Nociforo, N. Pietralla, D. Ralet, M. Reese, and V. Stepanov, *Nuclear Instruments and Methods in Physics Research Section A: Accelerators, Spectrometers, Detectors and Associated Equipment*, **736**, 81–87 (2014).
- [19] Y. Togano, T. Nakamura, Y. Kondo, M. Shikata, T. Ozaki, A.T. Saito, T. Tomai, M. Yasuda, H. Yamada, N. Chiga, H. Otsu, V. Panin, Y. Zaihong, and Y. Fujino, *Nuclear Instruments and Methods in Physics Research Section B: Beam Interactions with Materials and Atoms*, **463**, 195–197 (2020).
- [20] Junki Tanaka, Zaihong Yang, Stefan Typel, Satoshi Adachi, Shiwei Bai, Patrik van Beek, Didier Beaumel, Yuki Fujikawa, Jiaying Han, Sebastian Heil, et al., *Science*, **371**(6526), 260–264 (2021).
- [21] P.J Li, D Beaumel, J Lee, M Assié, S Chen, S Franchoo, J Gibelin, F Hammache, T Harada, Y Kanada-En'yo, et al., *Physical review letters*, **131**(21), 212501 (2023).
- [22] Y Matsuda, H Sakaguchi, J Zenihiro, S Ishimoto, S Suzuki, H Otsu, T Ohnishi, H Takeda, K Ozeki, K Tanaka, et al., *Nuclear Instruments and Methods in Physics Research Section A: Accelerators, Spectrometers, Detectors and Associated Equipment*, **643**(1), 6–10 (2011).
- [23] S Chebotaryov, S Sakaguchi, T Uesaka, T Akieda, Y Ando, M Assie, D Beaumel, N Chiga, M Dozono, Alfredo Galindo-Uribarri, et al., *Progress of Theoretical and Experimental Physics*, **2018**(5), 053D01 (2018).
- [24] Y Matsuda, H Sakaguchi, H Takeda, S Terashima, J Zenihiro, T Kobayashi, T Murakami, Y Iwao, T Ichihara, T Suda, et al., *Physical Review C*, **87**(3), 034614 (2013).
- [25] G Verde, L Acosta, Triestino Minniti, F Amorini, Lucrezia Auditore, R Bassini, C Boiano, G Cardella, A Chbihi, E De Filippo, et al., *The farcos project: femtoscope array for correlations and femtoscopy*, In *Journal of Physics: Conference Series*, volume 420, page 012158. IOP Publishing (2013).
- [26] J. Tanaka, R. Tsuji, K. Higuchi, H. Baba, M. Böhmer, T. Furuno, R. Gernhäuser, Y. Hijikata, S. Ishimoto, T. Kawabata, S. Kawase, Y. Kubota, S. Kurosawa, S. Takeshige, T. Uesaka, K. Yahiro, and J. Zenihiro, *Nuclear Instruments and Methods in Physics Research Section B: Beam Interactions with Materials and Atoms*, **542**, 4–6 (2023).
- [27] Ogata K Uesaka T., Zenihiro J., Grant-in-Aid for Specially Promoted Research (2021).
- [28] K. Higuchi, J. Tanaka, R. Tsuji, M. Böhmer, R. Gernhäuser, S. Kawase, J. Zenihiro, Y. Hijikata, R. Matsumura, K. Yahiro, S. Takeshige, H. Baba, E. Takada, and T. Uesaka, *Nuclear Instruments and Methods in Physics Research Section B: Beam Interactions with Materials and Atoms*, **542**, 84–86 (2023).
- [29] Pieter Doornenbal, *Progress of Theoretical and Experimental Physics*, **2012**(1), 03C004 (12 2012), <https://academic.oup.com/ptep/article-pdf/2012/1/03C004/11597694/pts076.pdf>.
- [30] P. Doornenbal, H. Scheit, N. Aoi, S. Takeuchi, K. Li, E. Takeshita, H. Wang, H. Baba, S. Deguchi, N. Fukuda, H. Geissel, R. Gernhäuser, J. Gibelin, I. Hachiuma, Y. Hara, C. Hinke, N. Inabe, K. Itahashi, S. Itoh, D. Kameda, S. Kanno, Y. Kawada, N. Kobayashi, Y. Kondo, R. Krücken, T. Kubo, T. Kuboki, K. Kusaka, M. Lantz, S. Michimasa, T. Motobayashi, T. Nakamura, T. Nakao, K. Namihira, S. Nishimura, T. Ohnishi, M. Ohtake, N. A. Orr, H. Otsu, K. Ozeki, Y. Satou, S. Shimoura, T. Sumikama, M. Takechi, H. Takeda, K. N. Tanaka, K. Tanaka, Y. Togano, M. Winkler, Y. Yanagisawa, K. Yoneda, A. Yoshida, K. Yoshida, and

- H. Sakurai, Phys. Rev. Lett., **103**, 032501 (Jul 2009).
- [31] P. Doornenbal, H. Scheit, S. Takeuchi, N. Aoi, K. Li, M. Matsushita, D. Steppenbeck, H. Wang, H. Baba, H. Crawford, C. R. Hoffman, R. Hughes, E. Ideguchi, N. Kobayashi, Y. Kondo, J. Lee, S. Michimasa, T. Motobayashi, H. Sakurai, M. Takechi, Y. Togano, R. Winkler, and K. Yoneda, Phys. Rev. Lett., **111**, 212502 (Nov 2013).
- [32] The SEASTAR project, <https://www.nishina.riken.jp/collaboration/SUNFLOWER/experiment/seastar/index.php> (2024).
- [33] RIBF Facility Upgrade Project, [https://www.nishina.riken.jp/researcher/RIBFupgrade/index\\_e.html](https://www.nishina.riken.jp/researcher/RIBFupgrade/index_e.html) (2024).
- [34] The HYPATIA array, <https://www.nishina.riken.jp/collaboration/SUNFLOWER/devices/hypatia/index.php> (2024).
- [35] A. Huck, G. Klotz, A. Knipper, C. Miehé, C. Richard-Serre, G. Walter, A. Poves, H. L. Ravn, and G. Marguier, Phys. Rev. C, **31**, 2226–2237 (Jun 1985).
- [36] F. Wienholtz, D. Beck, K. Blaum, Ch. Borgmann, M. Breitenfeldt, R. B. Cakirli, S. George, F. Herfurth, J. D. Holt, M. Kowalska, S. Kreim, D. Lunney, V. Manea, J. Menéndez, D. Neidherr, M. Rosenbusch, L. Schweikhard, A. Schwenk, J. Simonis, J. Stanja, R. N. Wolf, and K. Zuber, Nature, **498**(7454), 346–349 (Jun 2013).
- [37] S. Michimasa, M. Kobayashi, Y. Kiyokawa, S. Ota, D. S. Ahn, H. Baba, G. P. A. Berg, M. Dozono, N. Fukuda, T. Furuno, E. Ideguchi, N. Inabe, T. Kawabata, S. Kawase, K. Kisamori, K. Kobayashi, T. Kubo, Y. Kubota, C. S. Lee, M. Matsushita, H. Miya, A. Mizukami, H. Nagakura, D. Nishimura, H. Oikawa, H. Sakai, Y. Shimizu, A. Stolz, H. Suzuki, M. Takaki, H. Takeda, S. Takeuchi, H. Tokieda, T. Uesaka, K. Yako, Y. Yamaguchi, Y. Yanagisawa, R. Yokoyama, K. Yoshida, and S. Shimoura, Phys. Rev. Lett., **121**, 022506 (Jul 2018).
- [38] A. Gade, R. V. F. Janssens, D. Bazin, R. Broda, B. A. Brown, C. M. Campbell, M. P. Carpenter, J. M. Cook, A. N. Deacon, D.-C. Dinca, B. Fornal, S. J. Freeman, T. Glasmacher, P. G. Hansen, B. P. Kay, P. F. Mantica, W. F. Mueller, J. R. Terry, J. A. Tostevin, and S. Zhu, Phys. Rev. C, **74**, 021302 (Aug 2006).
- [39] S. Chen, J. Lee, P. Doornenbal, A. Obertelli, C. Barbieri, Y. Chazono, P. Navrátil, K. Ogata, T. Otsuka, F. Raimondi, V. Somà, Y. Utsuno, K. Yoshida, H. Baba, F. Browne, D. Calvet, F. Château, N. Chiga, A. Corsi, M. L. Cortés, A. Delbart, J.-M. Gheller, A. Giganon, A. Gillibert, C. Hilaire, T. Isobe, J. Kahlbow, T. Kobayashi, Y. Kubota, V. Lapoux, H. N. Liu, T. Motobayashi, I. Murray, H. Otsu, V. Panin, N. Paul, W. Rodriguez, H. Sakurai, M. Sasano, D. Steppenbeck, L. Stuhl, Y. L. Sun, Y. Togano, T. Uesaka, K. Wimmer, K. Yoneda, N. Achouri, O. Aktas, T. Aumann, L. X. Chung, F. Flavigny, S. Franchoo, I. Gašparić, R.-B. Gerst, J. Gibelin, K. I. Hahn, D. Kim, T. Koiwai, Y. Kondo, P. Koseoglou, C. Lehr, B. D. Linh, T. Lokotko, M. MacCormick, K. Moschner, T. Nakamura, S. Y. Park, D. Rossi, E. Sahin, D. Sohler, P.-A. Söderström, S. Takeuchi, H. Törnqvist, V. Vaquero, V. Wagner, S. Wang, V. Werner, X. Xu, H. Yamada, D. Yan, Z. Yang, M. Yasuda, and L. Zanetti, Phys. Rev. Lett., **123**, 142501 (Sep 2019).
- [40] Alexandra Gade, Physics, **3**(4), 1226–1236 (2021).
- [41] B. Alex Brown, Physics, **4**(2), 525–547 (2022).
- [42] S. Chen, F. Browne, P. Doornenbal, J. Lee, A. Obertelli, Y. Tsunoda, T. Otsuka, Y. Chazono, G. Hagen, J.D. Holt, G.R. Jansen, K. Ogata, N. Shimizu, Y. Utsuno, K. Yoshida, N.L. Achouri, H. Baba, D. Calvet, F. Château, N. Chiga, A. Corsi, M.L. Cortés, A. Delbart, J.-M. Gheller, A. Giganon, A. Gillibert, C. Hilaire, T. Isobe, T. Kobayashi, Y. Kubota, V. Lapoux, H.N. Liu, T. Motobayashi, I. Murray, H. Otsu, V. Panin, N. Paul, W. Rodriguez, H. Sakurai, M. Sasano, D. Steppenbeck, L. Stuhl, Y.L. Sun, Y. Togano, T. Uesaka, K. Wimmer, K. Yoneda, O. Aktas, T. Aumann, L.X. Chung, F. Flavigny, S. Franchoo, I. Gasparic, R.-B. Gerst, J. Gibelin, K.I. Hahn, D. Kim, T. Koiwai, Y. Kondo, P. Koseoglou, C. Lehr, B.D. Linh, T. Lokotko, M. MacCormick, K. Moschner, T. Nakamura, S.Y. Park, D. Rossi, E. Sahin, P.-A. Söderström, D. Sohler, S. Takeuchi, H. Törnqvist, V. Vaquero, V. Wagner, S. Wang, V. Werner, X. Xu, H. Yamada, D. Yan, Z. Yang, M. Yasuda, and L. Zanetti, Physics Letters B, **843**, 138025 (2023).
- [43] M.L. Cortés, W. Rodriguez, P. Doornenbal, A. Obertelli, J.D. Holt, S.M. Lenzi, J. Menéndez, F. Nowacki, K. Ogata, A. Poves, T.R. Rodríguez, A. Schwenk, J. Simonis, S.R. Stroberg, K. Yoshida, L. Achouri, H. Baba, F. Browne, D. Calvet, F. Château, S. Chen, N. Chiga, A. Corsi, A. Delbart, J.-M. Gheller, A. Giganon, A. Gillibert, C. Hilaire, T. Isobe, T. Kobayashi, Y. Kubota, V. Lapoux, H.N. Liu, T. Motobayashi, I. Murray, H. Otsu, V. Panin, N. Paul, H. Sakurai, M. Sasano, D. Steppenbeck, L. Stuhl, Y.L. Sun, Y. Togano, T. Uesaka, K. Wimmer, K. Yoneda, O. Aktas, T. Aumann, L.X. Chung, F. Flavigny, S. Franchoo, I. Gašparić, R.-B. Gerst, J. Gibelin, K.I. Hahn, D. Kim, T. Koiwai, Y. Kondo, P. Koseoglou, J. Lee, C. Lehr, B.D. Linh, T. Lokotko, M. MacCormick, K. Moschner, T. Nakamura, S.Y. Park, D. Rossi, E. Sahin, D. Sohler, P.-A. Söderström, S. Takeuchi, H. Toernqvist, V. Vaquero, V. Wagner, S. Wang, V. Werner, X. Xu, H. Yamada, D. Yan, Z. Yang, M. Yasuda, and L. Zanetti, Physics Letters B, **800**, 135071 (2020).
- [44] S. Paschalis, I.Y. Lee, A.O. Macchiavelli, C.M. Campbell, M. Cromaz, S. Gros, J. Pavan, J. Qian, R.M. Clark, H.L. Crawford, D. Doering, P. Fallon, C. Lionberger, T. Loew, M. Petri, T. Stezelberger, S. Zimmermann,

- D.C. Radford, K. Lagergren, D. Weisshaar, R. Winkler, T. Glasmacher, J.T. Anderson, and C.W. Beausang, *Nuclear Instruments and Methods in Physics Research Section A: Accelerators, Spectrometers, Detectors and Associated Equipment*, **709**, 44–55 (2013).
- [45] S. Akkoyun, A. Algora, B. Alikhani, F. Ameil, G. de Angelis, L. Arnold, A. Astier, A. Ataç, Y. Aubert, C. Aufranc, A. Austin, S. Aydin, F. Azaiez, S. Badoer, D.L. Balabanski, D. Barrientos, G. Baulieu, R. Baumann, D. Bazzacco, F.A. Beck, T. Beck, P. Bednarczyk, M. Bellato, M.A. Bentley, G. Benzoni, R. Berthier, L. Berti, R. Beunard, G. Lo Bianco, B. Birkenbach, P.G. Bizzeti, A.M. Bizzeti-Sona, F. Le Blanc, J.M. Blasco, N. Blasi, D. Bloor, C. Boiano, M. Borsato, D. Bortolato, A.J. Boston, H.C. Boston, P. Bourgault, P. Boutachkov, A. Bouty, A. Bracco, S. Brambilla, I.P. Brawn, A. Brondi, S. Broussard, B. Bruyneel, D. Bucurescu, I. Burrows, A. Bürger, S. Cabaret, B. Cahan, E. Calore, F. Camera, A. Capsoni, F. Carrió, G. Casati, M. Castoldi, B. Cederwall, J.-L. Cercus, V. Chambert, M. El Chambit, R. Chapman, L. Charles, J. Chavas, E. Clément, P. Cocconi, S. Coelli, P.J. Coleman-Smith, A. Colombo, S. Colosimo, C. Commeaux, D. Conventi, R.J. Cooper, A. Corsi, A. Cortesi, L. Costa, F.C.L. Crespi, J.R. Cresswell, D.M. Cullen, D. Curien, A. Czermak, D. Delbourg, R. Depalo, T. Descombes, P. Désesquelles, P. Detistov, C. Diarra, F. Didierjean, M.R. Dimmock, Q.T. Doan, C. Domingo-Pardo, M. Doncel, F. Dorangeville, N. Dosme, Y. Drouen, G. Duchêne, B. Dulny, J. Eberth, P. Edelbruck, J. Egea, T. Engert, M.N. Erduran, S. Ertürk, C. Fanin, S. Fantinel, E. Farnea, T. Faul, M. Filliger, F. Filmer, Ch. Finck, G. de France, A. Gadea, W. Gast, A. Geraci, J. Gerl, R. Gernhäuser, A. Giannatiempo, A. Giaz, L. Gibelin, A. Givechev, N. Goel, V. González, A. Gottardo, X. Grave, J. Grebosz, R. Griffiths, A.N. Grint, P. Gros, L. Guevara, M. Gulmini, A. Görgen, H.T.M. Ha, T. Habermann, L.J. Harkness, H. Harroch, K. Hauschild, C. He, A. Hernández-Prieto, B. Hervieu, H. Hess, T. Hüyük, E. Ince, R. Isocrate, G. Jaworski, A. Johnson, J. Jolie, P. Jones, B. Jonson, P. Joshi, D.S. Judson, A. Jungclaus, M. Kaci, N. Karkour, M. Karolak, A. Kaşkaş, M. Kebbiri, R.S. Kempley, A. Khaplanov, S. Klupp, M. Kogimtzis, I. Kojouharov, A. Korichi, W. Korten, Th. Kröll, R. Krücken, N. Kurz, B.Y. Ky, M. Labiche, X. Lafay, L. Lavergne, I.H. Lazarus, S. Leboutelier, F. Lefebvre, E. Legay, L. Legeard, F. Lelli, S.M. Lenzi, S. Leoni, A. Lermilage, D. Lersch, J. Leske, S.C. Letts, S. Lhenoret, R.M. Lieder, D. Linget, J. Ljungvall, A. Lopez-Martens, A. Lotodé, S. Lunardi, A. Maj, J. van der Marel, Y. Mariette, N. Marginean, R. Marginean, G. Maron, A.R. Mather, W. Mezczyński, V. Mendéz, P. Medina, B. Melon, R. Menegazzo, D. Mengoni, E. Merchan, L. Mihailescu, C. Michelagnoli, J. Mierzejewski, L. Milechina, B. Million, K. Mitev, P. Molini, D. Montanari, S. Moon, F. Morbiducci, R. Moro, P.S. Morrall, O. Möller, A. Nannini, D.R. Napoli, L. Nelson, M. Nespolo, V.L. Ngo, M. Nicoletto, R. Nicolini, Y. Le Noa, P.J. Nolan, M. Norman, J. Nyberg, A. Obertelli, A. Olariu, R. Orlandi, D.C. Oxley, C. Özben, M. Ozille, C. Oziol, E. Pachoud, M. Palacz, J. Palin, J. Pancin, C. Parisel, P. Pariset, G. Pascovici, R. Peghin, L. Pellegrini, A. Perego, S. Perrier, M. Petcu, P. Petkov, C. Petrache, E. Pierre, N. Pietralla, S. Pietri, M. Pignanelli, I. Piqueras, Z. Podolyak, P. Le Pouhalec, J. Pouthas, D. Pugnère, V.F.E. Pucknell, A. Pullia, B. Quintana, R. Raine, G. Rainovski, L. Ramina, G. Rampazzo, G. La Rana, M. Rebeschini, F. Recchia, N. Redon, M. Reese, P. Reiter, P.H. Regan, S. Riboldi, M. Richer, M. Rigato, S. Rigby, G. Ripamonti, A.P. Robinson, J. Robin, J. Roccaz, J.-A. Ropert, B. Rossé, C. Rossi Alvarez, D. Rosso, B. Rubio, D. Rudolph, F. Saillant, E. Şahin, F. Salomon, M.-D. Salsac, J. Salt, G. Salvato, J. Sampson, E. Sanchis, C. Santos, H. Schaffner, M. Schlarb, D.P. Scraggs, D. Seddon, M. Şenyiğit, M.-H. Sigward, G. Simpson, J. Simpson, M. Slee, J.F. Smith, P. Sona, B. Sowicki, P. Spolaore, C. Stahl, T. Stanios, E. Stefanova, O. Stézowski, J. Strachan, G. Suliman, P.-A. Söderström, J.L. Tain, S. Tanguy, S. Tashenov, Ch. Theisen, J. Thornhill, F. Tomasi, N. Toniolo, R. Touzery, B. Travers, A. Triossi, M. Tripon, K.M.M. Tun-Lanoë, M. Turcato, C. Unsworth, C.A. Ur, J.J. Valiente-Dobon, V. Vandone, E. Vardaci, R. Venturelli, F. Veronese, Ch. Veysiere, E. Viscione, R. Wadsworth, P.M. Walker, N. Warr, C. Weber, D. Weisshaar, D. Wells, O. Wieland, A. Wiens, G. Wittwer, H.J. Wollersheim, F. Zocca, N.V. Zamfir, M. Ziebliński, and A. Zucchiatti, *Nuclear Instruments and Methods in Physics Research Section A: Accelerators, Spectrometers, Detectors and Associated Equipment*, **668**, 26–58 (2012).
- [46] K. Wimmer, P. Doornenbal, N. Aoi, H. Baba, F. Browne, C. Campbell, H. Crawford, H. De Witte, C. Fransen, H. Hess, S. Iwazaki, J. Kim, A. Kohda, T. Koiwai, B. Mauss, B. Moon, T. Parry, P. Reiter, D. Suzuki, R. Taniuchi, S. Thiel, and Y. Yamamoto, *RIKEN Accel. Prog. Rep* 2020, **54**, S27 (2021).
- [47] Shinji Motomura, Shuichi Enomoto, Hiromitsu Haba, Kaori Igarashi, Yasuyuki Gono, and Yasushige Yano, *IEEE Transactions on Nuclear Science*, **54**(3), 710–717 (2007).
- [48] M.K. Suzuki, T. K. Onishi, H. J. Ong, H. Suzuki, Y. Ichikaw, N. Imai, N. Aoi, H. Iwasaki, and H. Sakurai, *RIKEN Accelerator Progress Report* 2003, **37**, 153 (2024).
- [49] K. Boretzky, M. Gašparić, M. Heil, J. Mayer, A. Heinz, C. Caesar, D. Kresan, H. Simon, H.T. Törnqvist, D. Körper, G. Alkharov, L. Atar, T. Aumann, D. Bemmerer, S.V. Bondarev, L.T. Bott, S. Chakraborty, M.I. Cherciu, L.V. Chulkov, M. Ciobanu, U. Datta, E. De Filippo, C.A. Douma, J. Dreyer, Z. Elekes, J. Enders, D. Galaviz, E. Geraci, B. Gnoffo, K. Göbel, V.L. Golovtsov, D. Gonzalez Diaz, N. Gruzinsky, T. Heftrich, H. Heggen, J. Hehner, T. Hensel, E. Hoemann, M. Holl, A. Horvat, Á. Horváth, G. Ickert, D. Jelavić Malenica,

- H.T. Johansson, B. Jonson, J. Kahlbow, N. Kalantar-Nayestanaki, A. Kelić-Heil, M. Kempe, K. Koch, N.G. Kozlenko, A.G. Krivshich, N. Kurz, V. Kuznetsov, C. Langer, Y. Leifels, I. Lihtar, B. Löher, J. Machado, N.S. Martorana, K. Miki, T. Nilsson, E.M. Orischin, E.V. Pagano, S. Pirrone, G. Politi, P.-M. Potlog, A. Rahaman, R. Reifarh, C. Rigollet, M. Röder, D.M. Rossi, P. Russotto, D. Savran, H. Scheit, F. Schindler, D. Stach, E. Stan, J. Stomvall Gill, P. Teubig, M. Trimarchi, L. Uvarov, M. Volkmandt, S. Volkov, A. Wagner, V. Wagner, S. Wranne, D. Yakorev, L. Zanetti, A. Zilges, and K. Zuber, Nuclear Instruments and Methods in Physics Research Section A: Accelerators, Spectrometers, Detectors and Associated Equipment, **1014**, 165701 (2021).
- [50] The EXPAND project, [https://www.in2p3.cnrs.fr/sites/institut\\_in2p3/files/page/2019-07/7-Doc-ORR.pdf](https://www.in2p3.cnrs.fr/sites/institut_in2p3/files/page/2019-07/7-Doc-ORR.pdf) (2019).
- [51] Y. Kondo N. A. Orr, J. Gibelin and H. Otsu for the NEBULA-Plus collaboration, RIKEN Accelerator Progress Report 2022, **56**, 91 (2023).
- [52] Marco Knoesel, *Measurement of the Neutron-Neutron Scattering Length*, PhD thesis, Technische Universitaet Darmstadt (2023).
- [53] T. Nakamura and R. Tanaka for the NEBULA Plus collaboration, Development of a next-generation neutron detector array HIME, [http://be.nucl.ap.titech.ac.jp/~ryuki/report/development\\_of\\_hime.pdf](http://be.nucl.ap.titech.ac.jp/~ryuki/report/development_of_hime.pdf) ().